Conductance of DNA molecules: Effects of decoherence and bonding

Matías Zilly,[1,*] Orsolya Ujsághy,[2,†] and Dietrich E. Wolf[1,*]
[1]*Department of Physics and CeNIDE, University of Duisburg–Essen, D-47048 Duisburg, Germany*
[2]*Department of Theoretical Physics and Condensed Matter Research Group of the Hungarian Academy of Sciences, Budapest University of Technology and Economics, Budafoki út 8., H-1521 Budapest, Hungary*
(Received 7 July 2010; revised manuscript received 2 September 2010; published 28 September 2010)

The influence of decoherence and bonding on the linear conductance of single double-stranded DNA molecules is examined by fitting a phenomenological statistical model developed recently [M. Zilly, O. Ujsághy, and D. E. Wolf, Eur. Phys. J. B **68**, 237 (2009)] to experimental results. The DNA molecule itself is described by a tight-binding ladder model with parameters obtained from published *ab initio* calculations [K. Senthilkumar, F. C. Grozema, C. F. Guerra, F. M. Bickelhaupt, F. D. Lewis, Y. A. Berlin, M. A. Ratner, and L. D. A. Siebbeles, J. Am. Chem. Soc. **127**, 14894 (2005)]. The good agreement with the experiments on sequence and length dependence gives a hint on the nature of conduction in DNA and at the same time provides a crucial test of the model.

DOI: 10.1103/PhysRevB.82.125125 PACS number(s): 87.14.gk, 73.63.−b, 87.15.Pc

I. INTRODUCTION

Motivated by molecular electronics and by the possibility to read out chemical and biological information electronically, transport through single double-stranded DNA molecules is a focus of current research in nanoscience. The experimental situation is not particularly clear. After the early investigations,[1] in the last 6 years increasing consensus emerged that DNA double strands with 8–26 base pairs are conducting. However, this conclusion may be misleading, as it depends on the chemical potential of the contacts, on the temperature, and on the coupling of DNA to the environment. The experiments are performed either in water[2–4] or in the dry state.[5,6] Moreover, all experiments show sequence-dependent conductance, which increases the more the (GC) content in the sample molecule dominates over the (AT) content. Sometimes ohmic behavior is reported, sometimes one finds an exponential decrease which is attributed to coherent tunneling. The change from coherent to ohmic behavior is usually attributed to the effect of decoherence caused by the water (e.g., Refs. 7–9), vibrational degrees of freedom,[10] or dynamical movement of the DNA bases.[11] Most of the theoretical studies perform model calculations,[12] but some of them present hybrid methods combining *ab initio* and molecular-dynamics studies,[8] sometimes also in combination with model calculations.[11]

The experiments clearly show that both the way, DNA is bonded, as well as the environment has an influence on the conductance. Here we present a calculation taking into account the effects of decoherence and bonding by extending a recently introduced phenomenological model.[13,14] It was originally developed for linear systems and adapting it to the quasilinear transport in DNA provides additional justification of the model.

As DNA Hamiltonian we use a realistic tight-binding model (the extended ladder model) based on *ab initio* calculations.[15–17] We investigate several sequences, for which experimental values for the conductance are known, in order to assess, how well they can be fitted by our model *without changing the microscopic energy values*, but just *adapting the four parameters* μ and Γ describing the coupling to the electrodes, and p and η describing the effect of decoherence (see Secs. III and IV).

The paper is organized as follows. In Sec. II we present the extended ladder model describing the double-stranded DNA. Section III is devoted to modeling the bonding to the electrodes according to the experimental situation. In Sec. IV we extend the statistical model for decoherence such that it becomes applicable to DNA. In Sec. V we compare our results to the experiments[2–4] and finally, we give our conclusions in Sec. VI.

II. EXTENDED LADDER MODEL OF DNA

The linear chain tight-binding model,[12] where each site corresponds to a base pair, is widely used in the literature to describe DNA. In some works also the backbone effects caused by the complementary strand and the sugar/phosphate mantle are taken into account (fishbone model).[12]

However, in order to account for arbitrary base sequences considering the correct base pairing, the so-called ladder model[12,18] is more appropriate. It consists of two coupled tight-binding chains corresponding to the two strands and each site represents a single base. There are calculations where backbone effects (here only due to the sugar/phosphate mantle) are considered in the ladder model, as well.[12] Since, according to *ab initio*[15–17] calculations the diagonal interstrand transfer matrix elements can be more relevant than the intrastrand coupling, we will use the extended ladder model of DNA (Refs. 15–17) sketched in Fig. 1.

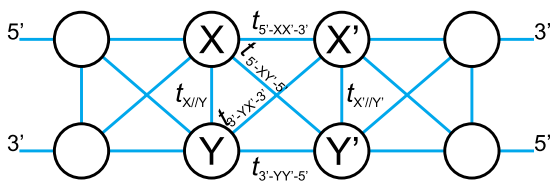

FIG. 1. (Color online) The extended ladder model for DNA double strands (Refs. 15–17).

 ©2010 The American Physical Society

TABLE I. The on-site energies and base pair couplings (in eV). On-site energies are averages of the values calculated by DFT (Ref. 15). They correspond to the HOMO orbitals at the respective bases.

ϵ_G	ϵ_A	ϵ_C	ϵ_T	$t_{G\|C}$	$t_{A\|T}$
8.178	8.631	9.722	9.464	−0.055	−0.047

The corresponding Hamiltonian describing a double-stranded DNA that is N base pairs long is

$$H = \sum_{i=1}^{N} \left[\sum_{m=1,2} \varepsilon_{i,m} c_{i,m}^{\dagger} c_{i,m} + \sum_{m,n=1,2;m\neq n} t_{i,mn} c_{i,m}^{\dagger} c_{i,n} + \sum_{m,n=1,2} t_{i,i+1,mn} (c_{i,m}^{\dagger} c_{i+1,n} + \text{H.c.}) \right], \quad (1)$$

where $c_{i,m}^{\dagger}$ creates a hole on strand m at the ith base pair with on-site energy $\varepsilon_{i,m}$. $t_{i,mn}$ and $t_{i,i+1,mn}$ are the base pair couplings and the hopping amplitudes between two bases of neighboring base pairs, respectively. The parameters used in the calculations for the on-site energies and the base pair couplings are listed in Table I. According to Ref. 15, the on-site energies calculated by density-functional theory (DFT) depend on the flanking nucleobases so that 16 different values were determined. For ϵ_G they vary between 7.890 and 8.407 eV, to give an idea. Also structural rearrangement (e.g., by shearing or twisting) of the DNA double strands causes shifts in the on-site energies of up to 1 eV.[19] Here, we want to propose a universal model, which can predict conductances for any sequence of base pairs. Within the model class, Eq. (1), a single value for the on-site energy of a nucleobase should be used. We simply take the average of the 16 values given in Ref. 15 for each nucleobase.

The hopping parameters (cf. Fig. 1) used in the calculation are listed in Table II. We use the single-strand notation, listing only the sequence of a single strand (the other strand is determined due to the unique base pairing). Because of the directionality of the DNA strands, $t_{5'\text{-}XY\text{-}3'} \neq t_{3'\text{-}XY\text{-}5'} = t_{5'\text{-}YX\text{-}3'}$ for $X \neq Y$. However, due to symmetry $t_{5'\text{-}XY\text{-}5'} = t_{5'\text{-}YX\text{-}5'}$ and $t_{3'\text{-}XY\text{-}3'} = t_{3'\text{-}YX\text{-}3'}$ for all X, Y.

Using the parameters given in Tables I and II the density of states for holes of an infinite DNA double strand is shown in Fig. 2. We can see two bands, one for holes with an energy around 8.2 eV and one around 9.7 eV. Each band is split into two subbands of width ≈0.04 eV. We prefer to describe the bands in terms of electrons in the following: the upper band at an energy −8.2 eV below the vacuum level and the lower one at −9.7 eV are both filled with electrons for an isolated neutral molecule.

TABLE II. Hopping parameters (in eV) for the extended ladder model, Fig. 1 (Ref. 15).

(a) $t_{5'\text{-}XY\text{-}3'} = t_{3'\text{-}YX\text{-}5'}$

	Y			
X	G	A	C	T
G	0.053	−0.077	−0.114	0.141
A	−0.010	−0.004	0.042	−0.063
C	0.009	−0.002	0.022	−0.055
T	0.018	−0.031	−0.028	0.180

(b) $t_{5'\text{-}XY\text{-}5'}$

G	0.012	−0.013	0.002	−0.009
A	−0.013	0.031	−0.001	0.007
C	0.002	−0.001	0.001	0.0003
T	−0.009	0.007	0.0003	0.001

(c) $t_{3'\text{-}XY\text{-}3'}$

G	−0.032	−0.011	0.022	−0.014
A	−0.011	0.049	0.017	−0.007
C	0.022	0.017	0.010	−0.004
T	−0.014	−0.007	−0.004	0.006

III. BONDING MODEL

Our aim is to examine the effect of the environment (decoherence) on the linear conductance of single double-stranded DNA molecules. We focus on the experiments in Refs. 2–4, where each gold electrode is coupled to a G base on the 3′ end via a thiol group. We model this as shown in Fig. 3, assuming wideband limit contacts attached only to the 3′ ends of the strands. The self-energies due to the left (L) and right (R) contacts are $2N \times 2N$ matrices, where all matrix elements are zero apart from the diagonal elements corresponding to $(i,m)=(1,2)$ on the left and $(i,m)=(N,1)$ on the right. These matrix elements are equal to the imaginary number $-i\Gamma/2$. We will consider the case of weak coupling to the

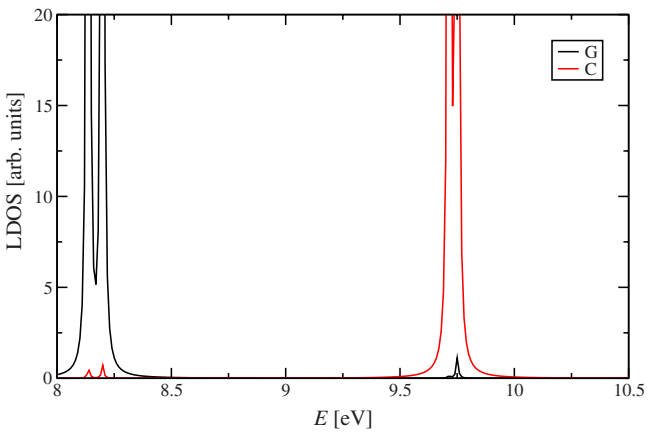

FIG. 2. (Color online) Density of states for holes, for 5′-$(CG)_\infty$-3′.

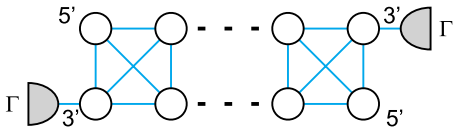

FIG. 3. (Color online) Extended ladder model, where only the 3′ ends of the strands are attached to the gold contacts via thiol-linker like in the experiments of Refs. 2–4.

electrodes, by choosing $\Gamma=0.003$ eV. This is of the same order of magnitude as the weakest hopping parameters in the DNA molecule.

The conductance of the DNA fragment depends also on the Fermi level of the contacts in relation to the DNA bands. Already a relative shift of 0.01 eV can significantly change the conductance. As the known values are hardly that reliable, we consider the chemical potential μ of the contacts as a fit parameter in the following. It must be kept in mind that μ denotes the chemical potential for holes. The one for electrons is given by $\mu_{\mathrm{el}}=-\mu$. We concentrate on values of μ_{el} within the immediate neighborhood of the uppermost occupied band, i.e., around −8.18 eV. Hence we describe the bonding of the DNA fragment by two fit parameters, the self-energy Γ and the chemical potential μ.

In Secs. IV and V we will calculate, how the linear conductance of the experimentally investigated sequences depends on these two bonding parameters. They should be the same for all sequences in Refs. 2–4, because the bonding was done the same way in all samples. We are going to use the recently developed phenomenological statistical method,[13,14] which takes decoherence into account by two further fit parameters.

IV. STATISTICAL MODEL FOR THE DECOHERENCE

The model is based on a different physical picture compared to other phenomenological descriptions of decoherence [like the method of fictitious reservoirs (Büttiker probes) (Ref. 20) or the method of Ref. 21]. Whereas there decoherence is continuously present in the sample, in our model it occurs only at stochastically distributed decoherence regions, where phase information gets completely lost.

We assume that decoherence can be described by local, stochastic events that couple a base pair (or part of it) to the environment. At those positions, phase coherence will be lost in both strands due to the interstrand couplings. In such a description the sequence consists of coherent sections separated by base pairs, on which decoherence events take place. The positions of the decoherence base pairs are chosen at random with a probability p giving rise to a particular decoherence configuration. The final results will be averaged over the different decoherence configurations. The average decoherence length is a/p,[13] where $a\approx 3.4$ Å is the distance between base pairs. p is the first of the two parameters characterizing decoherence in the model.

The coupling of a base pair to the environment implies that the local energy levels of the two bases will be broadened. In our model this broadening will be described by a parameter η. As we furthermore assume that coherence is

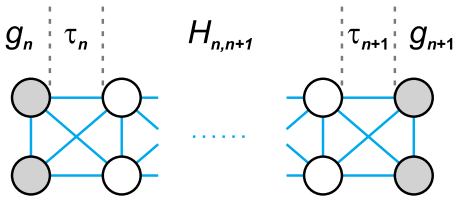

FIG. 4. (Color online) The transmission function of a coherent double-strand DNA molecule segment is calculated from the Hamiltonian given in Sec. II and the self-energies describing the connection to the decoherence base pairs at its ends (shaded).

completely destroyed on these base pairs, it makes sense to attribute a local energy distribution function to each decoherence base pair, which in general will differ from the Fermi distribution. Instead it will be a nonequilibrium distribution that emerges from the Fermi distributions $f_{\mathrm{L}}(E)$ and $f_{\mathrm{R}}(E)$ in the left, respectively, the right contact via the transmission of charge carriers through the coherent sections. We expect η to be larger than the broadening $\sim\Gamma/2$ due to the electrodes and of the same order of magnitude as the width of the subbands in Fig. 2 (≈ 0.04 eV).

The $(n-1)$st and the nth decoherence base pair can be regarded as "contacts" for the coherent section in between. The electrical current (and hence the conductance) can then be calculated according to the Landauer formula from the transmission function $T_{n-1,n}(E)$ of the coherent section and the energy distribution functions $f_{n-1}(E)$ and $f_n(E)$ at its boundaries,

$$I = 2\frac{e}{h}\int dE T_{n-1,n}(E)[f_{n-1}(E) - f_n(E)]. \tag{2}$$

The transmission functions for the coherent sections are calculated by applying the nonequilibrium Green's-function method[22] (see Fig. 4),

$$T_{n,n+1}(E) = 4\ \mathrm{Tr}[G_{n,n+1}(E)\mathrm{Im}\,\Sigma_{n+1}(E)G^{\dagger}_{n,n+1}(E)\mathrm{Im}\,\Sigma_n(E)], \tag{3}$$

where

$$G_{n,n+1}(E) = [E - H_{n,n+1} - \Sigma_n(E) - \Sigma_{n+1}(E)]^{-1} \tag{4}$$

is the Green's function of the segment between decoherence base pairs n and $n+1$. It is a matrix of dimension $2j_n\times 2j_n$, where j_n denotes the number of base pairs in the segment. The self-energy is a product of matrices

$$\underset{(2j_n\times 2j_n)}{\Sigma_n(E)} = \underset{(2j_n\times 2)}{\tau_n}\ \underset{(2\times 2)}{g_n(E)}\ \underset{(2\times 2j_n)}{\tau_n^{\dagger}} \tag{5}$$

with the dimensions given in the second line. τ_n is the coupling matrix connecting the segment to the decoherence base pair n (see Fig. 4). Its matrix elements can be identified from Fig. 1. The Green's function of the decoherence base pair n contains the corresponding Hamiltonian H_n and the coupling to the environment described in the simplest case by a constant imaginary self-energy $-i\eta$ (times the 2×2 unit matrix),

$$g_n(E) = [E - H_n + i\eta]^{-1}. \tag{6}$$

As we assume complete loss of phase information at the decoherence regions, one can write down master equations for the distribution functions, where the transfer rate of charge carriers between neighboring decoherence regions is proportional to the transmission function.[13] In the stationary state one obtains the following system of coupled linear equations:

$$T_{n-1,n}(E)[f_{n-1}(E) - f_n(E)] = T_{n,n+1}(E)[f_n(E) - f_{n+1}(E)]. \tag{7}$$

According to Eq. (2), Eq. (7) implies current conservation. They can be solved analytically,[13] using the boundary conditions $f_0(E)=f_L(E)$ and $f_{M+1}(E)=f_R(E)$, where M denotes the number of decoherence base pairs. Inserting the solution into Eq. (2) (e.g., for $n=M$) gives the current

$$I = 2\frac{e}{h}\int dE\left(\sum_{n=0}^{M}\frac{1}{T_{n,n+1}}\right)^{-1}[f_L(E) - f_R(E)]. \tag{8}$$

This leads to the linear conductance

$$G = G_0\int dE\left(\sum_{n=0}^{M}\frac{1}{T_{n,n+1}}\right)^{-1}\left(-\left.\frac{\partial f_{eq}}{\partial E}\right|_{\mu}\right), \tag{9}$$

where $G_0=2\frac{e^2}{h}$ is the conductance quantum (for the two spin channels), f_{eq} is the Fermi function, and μ is the equilibrium chemical potential of the contacts. For the results presented in the following, this expression has been averaged over typically 2000 independent decoherence configurations.

It is worth noting that temperature enters the result via several parameters. First, there is the explicit temperature dependence of the Fermi function. Moreover, the chemical potential μ and the decoherence parameters p and η implicitly depend on temperature.

Given the microscopic energy values in Tables I and II and the temperature, the model has four parameters. Two of them, μ and Γ, describe the coupling to the contacts. The other two are the decoherence parameters, p and η. As they describe a coupling to the environment, they may differ for dry and wet DNA, and they may also depend on the type of base pair.

V. RESULTS

In this section we present our results on the linear conductance for the sequences investigated experimentally in Refs. 2–4. The experimental data consist of conductance values for 5′-$(CG)_m$-3′ samples[2,4] with four different lengths [numbers of base pairs (nBPs) are $2m=8$, 10, 12, and 14], and for 5′-CGCG-$(A)_n(T)_n$-CGCG-3′ samples[2,3] with three different lengths (nBPs are $8+2n=8$, 10, and 12), where $n=0$ corresponds to the shortest 5′-$(CG)_{m=4}$-3′ sample.

We took the effect of finite temperature into account only in the Fermi functions of the electrodes. Since the experiments were performed at room temperature, we fixed $k_BT=0.0255$ eV. It is interesting to note, that in Ref. 4 experimentally unobservable temperature dependence was reported in the temperature range from 5 to 65 °C.

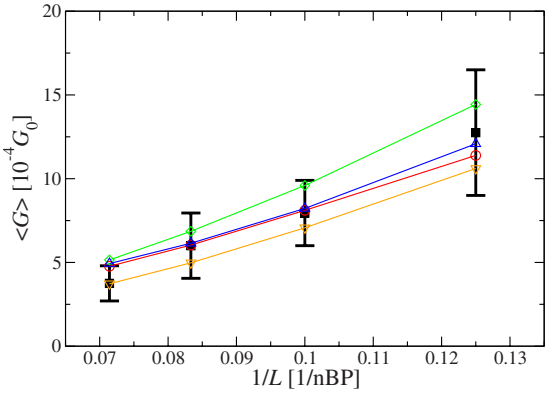

FIG. 5. (Color online) Calculated conductances for 5′-$(CG)_m$-3′ versus the inverse of the nBP $2m$ for parameter combinations ($\mu=8.07$ eV, $\eta=0.05$ eV) (red), ($\mu=8.18$ eV, $\eta=1.0$ eV) (blue), ($\mu=8.25$ eV, $\eta=0.05$ eV) (green), and ($\mu=8.26$ eV, $\eta=0.05$ eV) (orange). $\Gamma=0.003$ eV, $p=0.5$, and $k_BT=0.0255$ eV are the same for all curves. The experimental values (Refs. 2 and 4) are shown by ■ together with the error bars.

It is a hard task to investigate the whole four-dimensional parameter space of the model presented in Sec. IV. One needs to have reasonable guesses for the parameter values Γ, μ, p, and η. It turns out that the chemical potential μ of the electrodes is the most crucial parameter. Here we present data for four values, $\mu=8.07$ eV (μ_{el} slightly above the upper band), $\mu=8.18$ eV (μ_{el} within the upper band), and $\mu=8.25$ eV, respectively, $\mu=8.26$ eV (both μ_{el} slightly below the upper band of the isolated molecule). The coupling Γ to the electrodes is assumed to be of the same order of magnitude as the weakest hopping parameters in the DNA molecule. It is fixed to the value $\Gamma=0.003$ eV in all figures apart from the last one. As explained in Sec. IV, we regard values of η slightly larger than 0.04 eV (but still of the same order of magnitude) as reasonable. Finally, we guess that at room temperature a hole cannot travel ballistically further than perhaps two base pairs. Thus we choose $p=0.5$. These guesses will be confirmed by the results.

Figure 5 shows the measured conductances of four molecules of the type 5′-$(CG)_m$-3′, plotted versus the inverse of their length $L=2m$ (nBP).[2,4] Within the experimental error bars we obtained four excellent fits by keeping $p=0.5$ and $\Gamma=0.003$ eV fixed and optimizing η for each value of the chemical potential. The statistical errors of the calculated conductances are not shown in this figure for the sake of clarity. They are always less than half of the experimental errors. In the cases, where the chemical potential lies outside the band, the value $\eta=0.05$ eV led to good fits for all four data points. However, if the chemical potential lies inside the band, a good fit requires a value of $\eta=1$ eV, which seems unreasonably large.

Plotting the conductance as a function of inverse length suggests ohmic behavior. This is misleading, though, because a linear extrapolation would lead to vanishing conductance at a finite length. In Figs. 6–8 we plot the same data in a semilogarithmic way, showing that an exponential length dependence cannot be ruled out.

These figures also show two more experimental data points, which belong to molecules

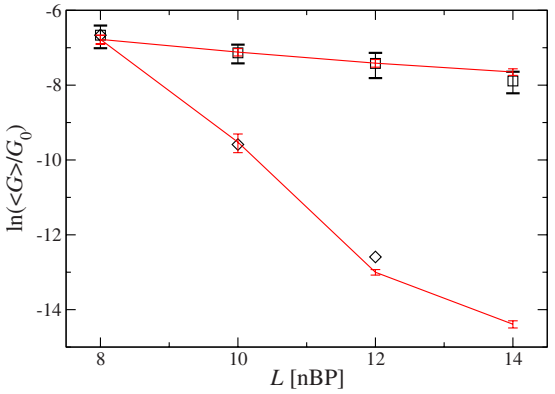

FIG. 6. (Color online) Conductance data for 5′-$(CG)_m$-3′ (□) (Refs. 2 and 4) and 5′-CGCG-$(A)_n(T)_n$-CGCG-3′ (◇) (Refs. 2 and 3) plotted semilogarithmically versus the nBP, $2m$, respectively, $8+2n$. For a value of μ=8.07 eV, our model fits both data sets, using the same parameters Γ=0.003 eV, p=0.5, and η=0.05 eV. k_BT=0.0255 eV.

5′-CGCG-$(A)_n(T)_n$-CGCG-3′ with n=1 and n=2. We calculated the corresponding conductances using the same parameters as obtained in Fig. 5 for the other molecules. Only the on-site energies and hopping parameters were adapted according to the Tables I and II. For the cases μ=8.07 eV, μ=8.25 eV, respectively, μ=8.26 eV excellent fits for the two new data points were obtained (see Figs. 6 and 8). However, for μ=8.18 eV, the new data points cannot be fitted with the old parameters. This casts further doubt on the validity of this parameter set, in addition to η being unreasonably large.

In the following we examine, how sensitively the calculated conductance for the longest of the 5′-$(CG)_m$-3′ samples (m=7) depends on the parameters η, p, and Γ. The purpose is to show that the values leading to the fits in Fig. 5 do not offer much freedom of choice, when varied individually. The chemical potential is fixed at μ=8.07 eV, μ=8.18 eV, respectively, μ=8.25 eV, corresponding to the fit curves close to the upper end of the error bar for this sample. It should be kept in mind, that a change in parameters that

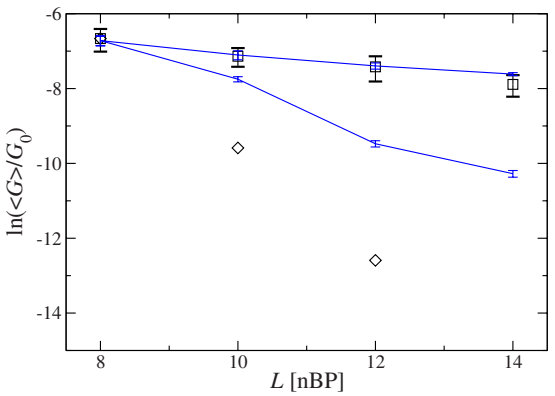

FIG. 7. (Color online) Same experimental data as in Fig. 6. For a value of μ=8.18 eV, the parameter values fitting 5′-$(CG)_m$-3′, Γ=0.003 eV, p=0.5, η=1.0 eV, do not fit the data for the chains with AT inclusions, k_BT=0.0255 eV.

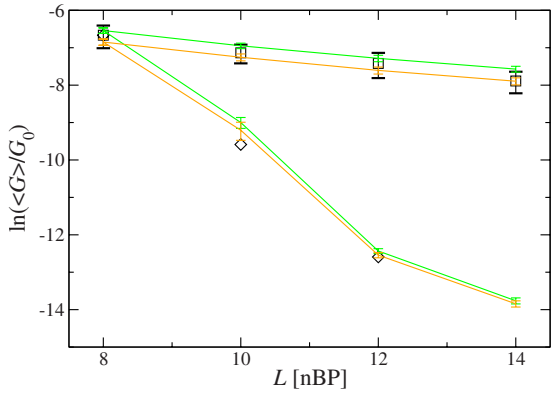

FIG. 8. (Color online) Same experimental data as in Fig. 6. For values between μ=8.25 eV (green) and μ=8.26 eV (orange), our model fits both data sets using the same parameters Γ=0.003 eV, p=0.5, η=0.05 eV, and k_BT=0.0255 eV.

moves this conductance closer to the experimental value, will in general lead to worse fits for the other three samples in Fig. 5.

In Fig. 9 the calculated conductance is plotted as a function of η while keeping p=0.5 and Γ=0.003 eV fixed on the values, for which the fits in Fig. 5 were obtained. For μ=8.07 eV and μ=8.25 eV the conductance does not depend sensitively on η: one would get acceptable fits for values in a large interval between 0.01 and 0.5 eV. This is true for a molecule that is 14 base pairs long. The optimization of the η value has to rely on the length dependence of the conductance. These data are crucial to narrow down the interval for this model parameter. By contrast, for μ=8.18 eV the conductance depends very sensitively on η, allowing acceptable fits only in a narrow interval around 1 eV and perhaps around a second value much below 0.01 eV. Both values are outside the range, which we regard as plausible.

In Fig. 10 the calculated conductance is plotted as a function of p while keeping η=0.05 eV, respectively, η=1 eV and Γ=0.003 eV fixed on the values giving the fits in Fig. 5.

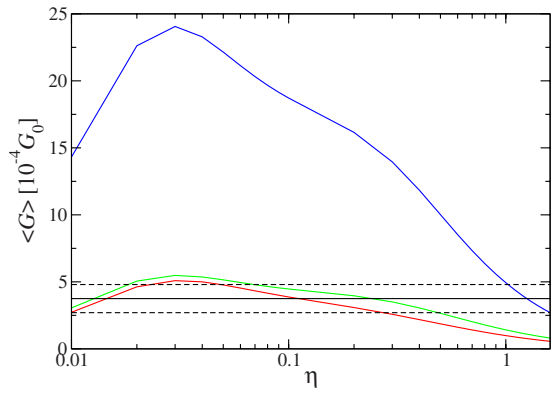

FIG. 9. (Color online) The sensitivity of the calculated conductance on η. The functions $G(\eta)$ are shown for μ=8.07 eV (red), μ=8.18 eV (blue), and μ=8.25 eV (green) for 5′-$(CG)_7$-3′. Γ=0.003 eV and p=0.5 are fixed. The experimental value is indicated by the horizontal full line, its error bar by the dashed ones. k_BT=0.0255 eV as in the experiment.

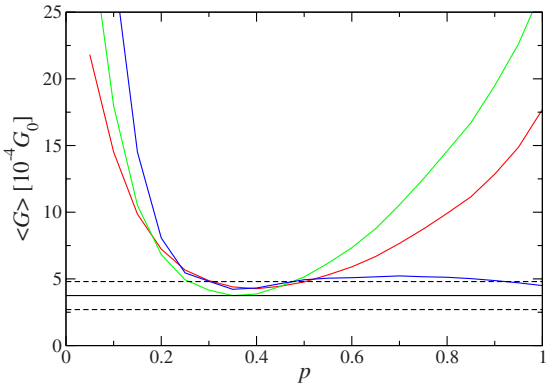

FIG. 10. (Color online) The sensitivity of the calculated conductance on p. The functions $G(p)$ are shown for $\mu=8.07$ eV, $\eta=0.05$ eV (red), $\mu=8.18$ eV, $\eta=1.0$ eV (blue), and $\mu=8.25$ eV, $\eta=0.05$ eV (green) for 5′-$(CG)_7$-3′. $\Gamma=0.003$ eV. The experimental value is indicated by the horizontal full line, its error bar by the dashed ones. $k_BT=0.0255$ eV as in the experiment.

For the chemical potentials outside the band [$\mu=8.07$ eV and $\mu=8.25$ eV] the sensitivity is high: only for p values in the interval between 0.3 and 0.5 one gets acceptable fits. However, for the chemical potential within the band ($\mu=8.18$ eV) the sensitivity is low: considering only the sample with 14 base pairs, any p value between 0.3 and 1 would be allowed.

In Fig. 11 the calculated conductance is plotted as a function of Γ while keeping $p=0.5$ and η fixed on the values giving the fits in Fig. 5. For all three chemical potentials the conductance depends sensitively on Γ. Acceptable fits are obtained between values somewhat below 0.001 and 0.003 eV, justifying our weak-coupling assumption. There may be a second fit interval with very large values above 1 eV, which we discard as implausible, because they would imply a coupling of the molecule to the electrodes that is better than any coupling between the base pairs within the molecule.

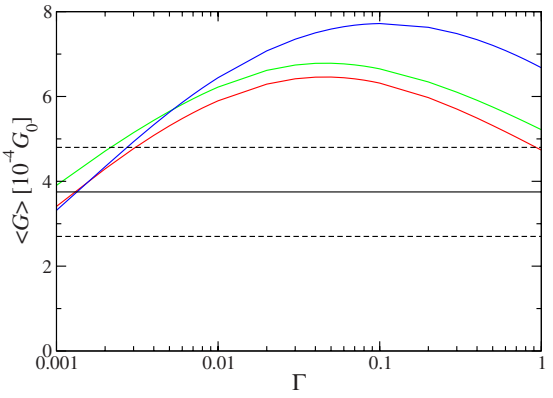

FIG. 11. (Color online) The sensitivity of the calculated conductance on Γ. The functions $G(\Gamma)$ are shown for $\mu=8.07$ eV, $\eta=0.05$ eV (red), $\mu=8.18$ eV, $\eta=1.0$ eV (blue), and $\mu=8.25$ eV, $\eta=0.05$ eV (green) for 5′-$(CG)_7$-3′. $p=0.5$. The experimental value is indicated by the horizontal full line, its error bar by the dashed ones. $k_BT=0.0255$ eV as in the experiment.

VI. CONCLUSIONS AND OUTLOOK

We have proposed a simple model in order to calculate the conductance of DNA-double-strand molecules for any sequence of base pairs. It is a tight-binding model with on-site energies and charge-transfer integrals taken from the DFT calculations in Ref. 15.

The on-site energies correspond to the energy difference between the vacuum level and the highest occupied molecular orbital (HOMO) of the nucleobase. In the 5′-$(CG)_\infty$-3′ double strand they give rise to a lower band about 9.72 eV, and an upper band about 8.18 eV below the vacuum level. Both of them are filled, if the molecule is neutral. The energy to create an electron-hole pair in such a molecule is on the order of $\min(\mathrm{LUMO_C},\mathrm{LUMO_G})+8.18$ eV$\approx 3-4$ eV,[1] where $\mathrm{LUMO_{C/G}}$ denotes the energy of the lowest unoccupied molecular orbital of C, respectively, G. Actually the difference between the band centers overestimates the band gap, but as the bandwidth is on the order of 0.05 eV, the conclusion is still correct that thermal activation of charge carriers at room temperature can be ruled out.

The situation changes, if the DNA molecule is brought into contact with gold electrodes. Let us first discuss the case, where the chemical potential of holes in the electrode is $\mu=8.07$ eV (in other words, electronic states are filled up to the energy −8.07 eV). At room temperature there will be thermally activated holes in the electrode down to the $\mathrm{HOMO_G}$ level. They can be injected into the molecule and carry a current through the molecule. In this sense the electrode has a similar effect as acceptors in a p-doped semiconductor. This works only, if the molecule is short enough that no localized space charges form at the contacts. In summary, for $\mu=8.07$ eV the molecule is a hole conductor, which remains neutral when contacted.

If the chemical potential of holes in the electrode is $\mu=8.26$ eV, we obtained fits of the experimental data of similar quality. In this case, however, the Fermi energy of the gold electrodes lies below the uppermost filled band of the DNA molecule. Again we assume that the molecule is short enough that space charges extend all the way from one side to the other. Then the upper band will be depleted, the molecule will carry a positive charge of $2N$ elementary charges, where N is the number of base pairs. In the electrodes there will be thermally activated electrons reaching up to the now empty $\mathrm{HOMO_G}$ level. In this case the electrodes act like donors in an n-doped semiconductor. In summary, for $\mu=8.26$ eV the molecule would become charged when contacted, and it would be an electron conductor.

The third parameter set, for which we could find an excellent fit of the conductance of 5′-$(CG)_n$-3′ double strands, had $\mu=8.18$ eV, which lies within the upper occupied band of the DNA molecule. This will lead to a depletion of the band, which is only partial, so that no thermal activation of charge carriers is needed. In this sense the DNA molecule behaves like a metal, provided it is shorter than the screening length. However, the fit requires a decoherence induced level broadening $\eta=1$ eV, which is unphysically large. Moreover, the same parameter set is incompatible with the conductance data for the mixed 5′-CGCG-$(A)_n$-$(T)_n$-CGCG-3′ double strands. Therefore, this scenario can be ruled out.

Most of the experimental and the theoretical examinations refer to hole conduction. Therefore we can conclude that the first parameter set (μ=8.07 eV, η=0.05 eV, Γ=0.003 eV, and p=0.5) is the most plausible one to describe the DNA molecules considered.

Summarizing, we extended our phenomenological model[13,14] for describing the effect of decoherence in double stranded DNA molecules. We could fit all of the experimental data of Refs. 2–4 without changing the microscopic energy values and by using the same parameter set of the model. For other experimentally investigated sequences[5,6] work is in progress.

ACKNOWLEDGMENTS

We would like to thank N. J. Tao for helpful information on the details of their experiments. This work was supported by DFG under Grant No. GRK 1240 "Nanotronics." O.U. acknowledges the support of the Alexander von Humboldt Foundation and the János Bolyai Research Foundation of the Hungarian Academy of Sciences.

*http://www.uni-due.de/comphys
†ujsaghy@neumann.phy.bme.hu

[1] For a summary, see R. G. Endres, D. L. Cox, and R. R. P. Singh, Rev. Mod. Phys. **76**, 195 (2004).
[2] B. Xu, P. Zhang, X. Li, and N. Tao, Nano Lett. **4**, 1105 (2004).
[3] J. Hihath, B. Xu, P. Zhang, and N. Tao, Proc. Natl. Acad. Sci. U.S.A. **102**, 16979 (2005).
[4] J. Hihath, F. Chen, P. Zhang, and N. Tao, J. Phys.: Condens. Matter **19**, 215202 (2007).
[5] A. K. Mahapatro, K. J. Jeong, G. U. Lee, and D. B. Janes, Nanotechnology **18**, 195202 (2007).
[6] D. Dulić, S. Tuukkanen, C.-L. Chung, A. Isambert, P. Lavie, and A. Filoramo, Nanotechnology **20**, 115502 (2009).
[7] R. Gutiérrez, S. Mandal, and G. Cuniberti, Nano Lett. **5**, 1093 (2005).
[8] S. S. Mallajosyula, J. C. Lin, D. L. Cox, S. K. Pati, and R. R. P. Singh, Phys. Rev. Lett. **101**, 176805 (2008).
[9] E. B. Starikov, A. Quintilla, C. Nganou, K. H. Lee, G. Cuniberti, and W. Wenzel, Chem. Phys. Lett. **467**, 369 (2009).
[10] B. B. Schmidt, M. H. Hettler, and G. Schön, Phys. Rev. B **77**, 165337 (2008); **75**, 115125 (2007).
[11] R. Gutiérrez, R. A. Caetano, B. P. Woiczikowski, T. Kubar, M. Elstner, and G. Cuniberti, Phys. Rev. Lett. **102**, 208102 (2009).
[12] For a review of the tight-binding models used to describe transport in DNA, see G. Cuniberti, E. Maciá, A. Rodriguez, and R. A. Römer, in *Charge Migration in DNA: Perspectives from Physics, Chemistry and Biology, NanoScience and Technology*, edited by T. Chakraborty (Springer, Berlin, 2007), Chap. 1, pp. 1–20.
[13] M. Zilly, O. Ujsághy, and D. E. Wolf, Eur. Phys. J. B **68**, 237 (2009).
[14] M. Zilly, Ph.D. thesis, University of Duisburg-Essen, 2010.
[15] K. Senthilkumar, F. C. Grozema, C. F. Guerra, F. M. Bickelhaupt, F. D. Lewis, Y. A. Berlin, M. A. Ratner, and L. D. A. Siebbeles, J. Am. Chem. Soc. **127**, 14894 (2005).
[16] T. Kubař, P. B. Woiczikowski, G. Cuniberti, and M. Elstner, J. Phys. Chem. B **112**, 7937 (2008).
[17] H. Zhang, X.-Q. Li, P. Han, X. Y. Yu, and Y. Yan, J. Chem. Phys. **117**, 4578 (2002).
[18] J. H. Wei and K. S. Chan, J. Phys.: Condens. Matter **19**, 286101 (2007).
[19] S. S. Mallajosyula and S. K. Pati, J. Phys. Chem. Lett. **1**, 1881 (2010).
[20] M. Büttiker, Phys. Rev. B **33**, 3020 (1986); J. L. D'Amato and H. M. Pastawski, *ibid.* **41**, 7411 (1990).
[21] R. Golizadeh-Mojarad and S. Datta, Phys. Rev. B **75**, 081301 (2007).
[22] S. Datta, *Electronic Transport in Mesoscopic Systems* (Cambridge University Press, Cambridge, England, 1997); *Quantum Transport: Atom to Transistor* (Cambridge University Press, Cambridge, England, 2005).